**ORIGINAL PAPER**

# Thermochemical conversion characteristics and kinetics of Cu- and Mn-contaminated biomass using a continuous pyrolysis-combustion method

X. Wang[1,2,5] · Y. Shao[3] · H. Wang[4] · B. Jin[2]

## Abstract

Phytoremediation technology has been well developed in the remediation of heavy metal pollution due to its low cost, in-situ disposal, permanent treatment, and environmental friendliness. The harvested phytoremediation plants are the combustible solid wastes and the disposal of them has drawn much attention. To realize clean disposal and utilization of Cu- and Mn-polluted plants, a two-stage thermochemical conversion technology combining pyrolysis and combustion was developed. In the continuous heating process, the pyrolysis characteristics at different final temperatures and combustion products of pyrolysis residual were analyzed in TG-MS and fixed bed reactor. Using the Coats-Redfern method, different kinetic models were tried to fit the pyrolysis process. It is demonstrated that these models can not be used to fit the whole pyrolysis and the kinetic parameters showed obvious segmentation characteristics. Apparent activation energies in the second and third stages during pyrolysis are 39.73–42.04 kJ/mol and 2.20–4.78 kJ/mol respectively. Additionally, experimental results exhibited that the weight loss rate increases from 62.5% to 66.2% when the pyrolysis temperature increases from 450 °C to 600 °C. Meanwhile, the retention ratio of Cu decreases from 64.6% to 26.4% while the ratio of Mn decreases from 58.8% to 34.4%.

**Keywords** Cu/Mn-contaminated biomass · Pyrolysis · Combustion · Kinetics · Retention behavior

Editorial responsibility: S. Mirkia.

✉ X. Wang
wangxd@njtech.edu.cn

1 Jiangsu Key Laboratory of Process Enhancement & Energy Equipment Technology, School of Mechanical and Power Engineering, Nanjing Tech University, Nanjing 211816, China

2 Key Laboratory of Energy Thermal Conversion and Control of Ministry of Education, School of Energy and Environment, Southeast University, Nanjing 210096, China

3 Engineering Laboratory for Energy System Process Conversion & Emission Control Technology of Jiangsu Province, School of Energy and Mechanical Engineering, Nanjing Normal University, Nanjing, China

4 China Resources Building Materials Technology Holdings Co.,Ltd, Shenzhen 518000, Guangdong, China

5 Sinoma International Engineering Co., Ltd., 211100 Nanjing, China

## Introduction

Heavy metal pollution has been a serious global environmental problem (Hou et al. 2020; Wu et al. 2022; He et al. 2023). Phytoremediation technology for accumulating heavy metals has been one promising way to overcome pollution (Shah and Daverey 2020; Wang et al. 2023a). In this circumstance, disposal of heavy-metal-contaminated biomass becomes a key problem to avoid secondary environmental pollution. On the other hand, the global energy demand issue is faced for sustainable development. As the nature of the contaminated plant is renewable biomass, the feasibility of contaminated biomass as an alternative fuel has been focused on recently (Wiangkham and Prapagdee 2018; Zeng et al. 2019; Tran et al. 2020; Lee and Park 2021).

There are different ways for the conversion and utilization of heavy-metal-contaminated biomass, such as heat treatment, extraction treatment, microbial treatment, compression landfill, and so on (Du et al. 2019; Liu and Tran 2021; Wang et al. 2022, 2023b; Amabogha et al. 2023). Thermochemical conversion has favorable performances due to the reason that it can reduce weight and volume significantly.

Meanwhile, the carbon resource in the contaminated biomass is efficiently utilized.

Regular thermochemical ways are combustion, gasification, and pyrolysis (Kovacs and Szemmelveisz 2017; Chai et al. 2022). The combustion and gasification are always performed in oxidative atmosphere while pyrolysis is conducted under inert conditions. Among the thermochemical methods, pyrolysis can be operated under relatively low temperatures. Its fundamental mechanism is carbonization of the biomass materials under anoxic condition and hampering the flame ignition. And the pyrolysis products are usually biochar, bio-oil, and combustible gases, which can be further used as fuel or valuable material. Therefore, pyrolysis is considered an efficient method for resource recovery and clean treatment of contaminated biomass, and it has been widely studied (Grottola et al. 2019; Liu et al. 2020; Zhang et al. 2020, 2021a).

During the pyrolysis process, the heavy metals in contaminated biomass may be distributed in gaseous, liquid, and solid phases. Lievens et al. (2008a, b) used contaminated *Maatheide* birch and sunflower as solid feedstocks to study the distribution of heavy metals (Cd, Cu, Pb, and Zn) in pyrolysis products at temperatures from 673 to 873 K. It is found that low temperature has a positive effect on the enrichment of heavy metals in biochar for all these heavy metals. Stals et al. (2010) studied the pyrolysis characteristics of Zn-, Cd-, Cu- and Pb-contained remediation plants using the flash pyrolysis method. Results showed that at 623 K and 723 K, the recovery of metals in char is approximately the same while it is much lower at 823 K. Pyrolysis of heavy-metal-contaminated *Avicennia marina* was conducted by He et al. (2019a). Though 12 kinds of heavy metals showed different migration properties at temperatures from 300 ℃ to 800 ℃, all of them tended to transform into volatile with the increase in temperature. Wang et al. (2017) studied the pyrolysis of *Phytolaccaceae*, a Mn-enriched plant, in a tubular furnace. When the pyrolysis temperature was 600 ℃, the leaching rate of Mn in the obtained biochar was only 0.15%, and more than 90% of other nonvolatile heavy metals were retained in the biochar. Fast pyrolysis was demonstrated to be an available method to control the quality of pyrolysis product. In the field of contaminated biomass dispose, Kuppens et al. (2015) found that fast pyrolysis in a fixed bed can effectively prevent the volatilization of heavy metals so that more heavy metals can be retained in biochar. Liu et al. (2012) investigated the fast pyrolysis performance of Cu-polluted biomass. It was found that Cu played a catalytic role in the pyrolysis process and it promoted bio-oil yield. Similar phenomena were also found in the pyrolysis of other heavy-metal-contaminated biomasses (Huang et al. 2018; Raheem et al. 2022). Zeng et al. (2019) used solar-assisted flash pyrolysis to study the effect of heavy metals on biogas. The results showed that after 5 min of pyrolysis of phytoremediation plants at 1200 ℃, the yields of $H_2$ and

CO were increased by 14.8% and 34.5% due to the presence of heavy metals Cu and Ni, respectively. Compared to uncontaminated biomass, He et al. (2019b) found that due to the catalytic role of heavy metals, both the biochar and gas yields were enhanced during the pyrolysis of contaminated biomass. As pyrolysis was affected by many factors, the operating conditions of pyrolysis can be adjusted and optimized to realize the immobilization of heavy metals in biochar. It is a common perspective that using low- or medium-temperature pyrolysis to treat contaminated biomass is beneficial for reducing the biological toxicity of contained heavy metals and the pyrolysis considerably suppresses the mobility and bioavailability of heavy metals in biochar (Liu et al. 2020).

As has been aforementioned, the pyrolysis products in different phases have their value. Usually, the pyrolysis gas and oil were used as fuel. However, a few works focus on the utilization of pyrolysis residual. It was found that the pyrolyzed biochar from some phytoremediation plants at high temperatures was environmentally acceptable with low risk (Zhang et al. 2021b). The pyrolyzed biochar is of high content of carbon, which is also a good resource of fuel. However, its utilization needs an understanding of the properties. To our best knowledge, it has not been investigated for continuous utilization of pyrolyzed biochar from phytoremediation plants as solid fuel.

Therefore, a two-stage disposal approach is proposed to investigate the conversion performances of the heavy-metal-contaminated biomass, aiming to realize the clean disposal of it. The two-stage method includes a pyrolysis period and a combustion process. As has been illustrated in literatures, pyrolysis can decrease the toxicity of heavy metals and produce available gases. The contaminated biomass was pyrolyzed under relatively low temperatures, and then the solid residual was burned to explore its behaviors. The main objective of this work is to study the feasibility of this two-stage thermochemical conversion method and identify the products during this process. The thermogravimetric-mass spectrometer (TG-MS) and fixed-bed reactor experiments were conducted to obtain the distribution of gaseous products and heavy metal behaviors respectively. Based on the experimental results, the pyrolysis kinetic parameters were determined. This work offers an efficient disposal method for heavy-metal-contaminated biomass.

# Materials and methods

## Experimental setup

The Cu- and Mn-contaminated biomass, *Phytolacca americana* L., was used as solid fuel. The pyrolysis and combustion performances of contaminated biomass were

investigated in a TG-MS and a fixed-bed reactor under different operating temperatures. In the two-stage thermochemical conversion experiment, nitrogen was used as the carrying gas for pyrolysis while the air was used during combustion process.

TG typed STA449 F3 (NETZSCH) was used to analyze the weight changes of samples while the gas product was analyzed by MS typed QMS 403D Aëolos (NETZSCH). The fixed-bed reactor is made of a quartz tube embedded in the stainless-steel body. The height and diameter of the quartz tube are 400 and 34 mm, respectively. A sintering plate of about 100 meshes is arranged 150 mm from the bottom of the reactor to place the sample. The experimental setups of TG-MS and fixed-bed reactor are shown in Fig. 1.

## Experimental operation method

In the TG-MS experiment, contaminated biomass sample with the mass of 12.00 mg was placed in an alumina crucible in each test and then it was put into the TG. After that, the pyrolysis-combustion experiment was carried out. First, the reaction area was purged using nitrogen (99.99%) for several minutes to guarantee that the pyrolysis was conducted in the atmosphere without oxygen. Then, the reaction area of the TG was heated in a nitrogen atmosphere with a heating rate of 10 °C/min. When it reached the final pyrolysis temperature in each test, the temperature was kept constant for 2 h. Next, the air with a purity of 99.99% was introduced

into the TG for the combustion of pyrolysis residual, and the heating rate was set at 10 °C/min simultaneously. When the temperature reached 900 °C, it was kept constant for 1 h aiming to the complete combustion of the sample. During the pyrolysis-combustion processes, the flowrate of nitrogen or air was set as 200 mL/min and a stream of nitrogen with a flowrate of 20 mL/min was used as protection gas.

The sample used in TG-MS is of low weight which makes it hard to analyze the content of heavy metals in pyrolyzed biochar. To overcome this problem, a pyrolysis experiment was conducted in a fixed-bed reactor to investigate the retention of heavy metals in biochar. In each test, 1.0000 g Cu- and Mn-contaminated biomass sample was placed in the fixed-bed reactor. For a sufficient gas–solid contact, the solid sample was put on a quartz wool layer located on the sintered plate. The nitrogen stream with a flowrate of 200 mL/min was introduced and the heating rate was also set at 10 °C/min for the pyrolysis experiment. When it reached the final pyrolysis temperature which was same as that in the TG-MS experiment, a 2-h constant temperature period lasted for a complete pyrolysis. Then, the reactor was cooled in a nitrogen atmosphere. This experiment has the same conditions as that using TG-MS. The obtained biochar was analyzed to measure the contents of Cu and Mn.

To obtain the content of heavy metals, the solid sample with a weight of about 0.070 g was used. Then it was added to the HCl and HNO$_3$ solution (10 mL) with a ratio of 1:3 for microwave-assisted digestion. While the digestion was
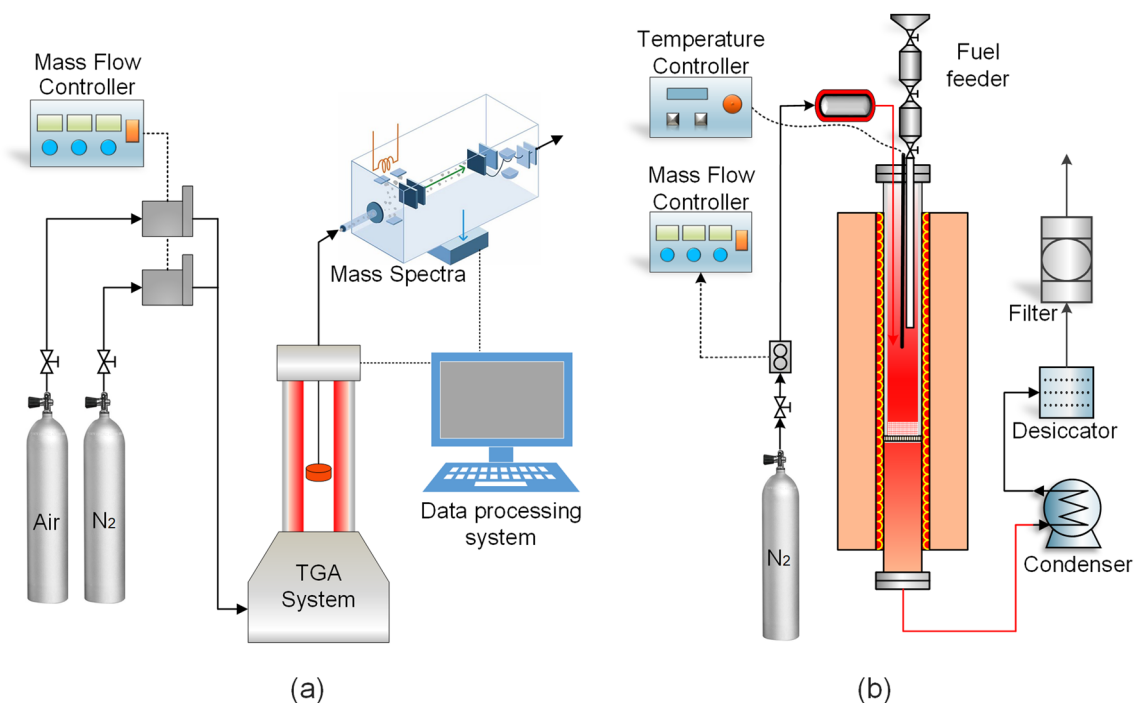


(a)                    (b)

**Fig. 1** Principal diagram of the TG-MS and fixed-bed reactor

completed, an inductively coupled plasma optical emission spectrometer (ICP-OES) typed Agilent 720ES was used to determine the content of heavy metals with an RF power of 1.20 kW. According to the measurement results, the content of heavy metals in the raw solid sample can be calculated.

## Solid materials

The contaminated biomass, *Phytolacca americana* L., used in this experiment was from Huanjiang, Guangxi. The raw material was naturally dried after harvest. Then, the contaminated biomass was crushed. The contaminated biomass powder with a particle size of 20–40 mesh was selected as solid feed in this experiment. The proximate analysis was conducted according to the national standard GB/T 28731–2012 of China. The ultimate analysis of the sample was measured using the analyzer produced by Elemantar (typed Vario EL cube). The ultimate and proximate analyses are given in Table 1.

The content of heavy metals in the raw biomass sample was calculated according to the ICP-OES measurement result. The Cu and Mn concentrations in the original sample are 17.05 mg/kg and 114.06 mg/kg.

## Results and discussion

### Thermogravimetric analysis during pyrolysis-combustion process

The pyrolysis and combustion were conducted in TG-MS. The effects of different final pyrolysis temperatures on the product were investigated. The final temperatures in different tests were set as 450, 500, 550, and 600 °C with the same heating rate of 10 °C/min, denoted as test1 to 4 respectively. After 2 h, the combustion process continued for a complete conversion of biochar. The thermogravimetric (TG) curve and derivative thermogravimetric (DTG) curve during these periods are shown in Fig. 2.

From the TG curve, it is seen that in the initial several minutes, the sample weights of contaminated biomass remained constant. With the increase in the temperature, the weights of samples show an obvious decrease with different rates during different periods. Accordingly, the first weight loss peak appears on the DTG curve with the maximum weight loss rate of about 1%/min. And it is seen the temperature at this peak is approximately 102 °C. This temperature
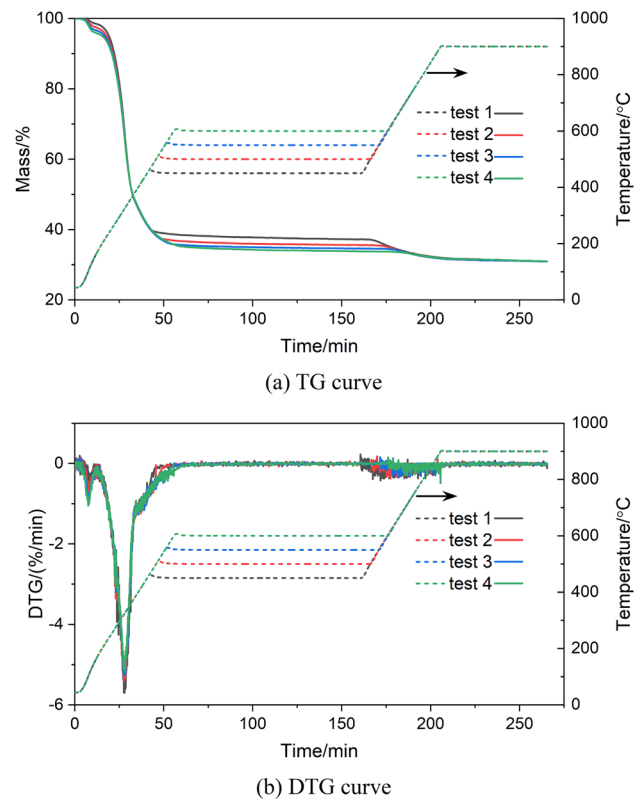


(a) TG curve



(b) DTG curve

**Fig. 2** TG and DTG curves of different tests during the pyrolysis-combustion process

is close to the evaporation temperature of the water, therefore it can be considered that the loss of free water in biomass samples reaches a peak value at this temperature.

When the temperature approaches 150 °C, the first DTG peak ends and the DTG value rises to around zero. The stage from the initial temperature to 150 °C is the loss stage of free water and chemically bound water. The second stage is in the temperature range of 150–400 °C, where the biomass sample loses weight rapidly and significantly. From the curve in the figure, it can be seen that the sample mass at this stage drops to approximately 40%, and hemicellulose and cellulose in the contaminated biomass are decomposed at this stage, which corresponds to the results by similar research (Sun et al. 2019). The maximum of weight loss rate in the DTG curve is close to 5.7%/min, and the peak appears in the range of 320–350 °C.

From 400 °C to different final pyrolysis temperatures in these tests, biomass samples continue to lose weight. During

**Table 1** Ultimate and proximate analyses of the contaminated biomass

| Proximate analysis (wt%, air dry basis) | | | | Ultimate analysis (wt%, dry basis) | | | |
|---|---|---|---|---|---|---|---|
| Moisture | Volatile | Fixed carbon | Ash | C | H | N | S |
| 9.71 | 63.34 | 21.30 | 5.65 | 43.43 | 6.99 | 1.05 | 0.29 |

this process, the degree of weight loss varies under different operating conditions. At high temperatures, the sample loses more weight. When the sample temperature reaches the set final pyrolysis temperature, the weight loss of the sample continues. From the DTG curve, it can be seen that after the temperature is maintained at the pyrolysis temperature for about 6–8 min, the weight of the sample does not change. This indicates that the pyrolysis of biomass samples at this temperature is complete. Scholars generally believe that when the temperature is higher than 400 °C, the main reaction during biomass pyrolysis is the polycondensation of biochar. Therefore, due to the limitation of pyrolysis temperature, the degree of polycondensation reaction varies at this stage. Final pyrolysis temperature is one of the important factors affecting biochar products. After 2-h isothermal pyrolysis, the sample quality decreases with the increase in temperature. The weights of biochar are 37.5%, 36.3%, 34.6%, and 33.8% when the final temperatures are 450, 500, 550 and 600 °C respectively. After the combustion process,

the sample weight has reached a stable level at 900 °C, and the final weight is consistent under different operating conditions.

## Analyses of the gaseous products during the pyrolysis-combustion process

In different periods of the pyrolysis-combustion process, the weight of the Cu- and Mn-contaminated biomass sample decreases against the temperature. Affected by pyrolysis temperature, pyrolysis products have divergent concentrations. TG-MS was used to clarify the gaseous products during different reaction stages. The mass-to-charge ratio of each gas is recorded as $m/z$, and gaseous products with $m/z = 2$ ($H_2$), 16 ($CH_4$), 17 ($NH_3$), 27 (HCN), 28 (CO, $N_2$), 30 (NO, $C_2H_4$) and 44 ($CO_2$, $C_3H_8$) are tested respectively. The use of $N_2$ as the carrier gas during the pyrolysis process affects the results of CO, therefore it is not further discussed. The analysis results of the gas phase are shown in Fig. 3.
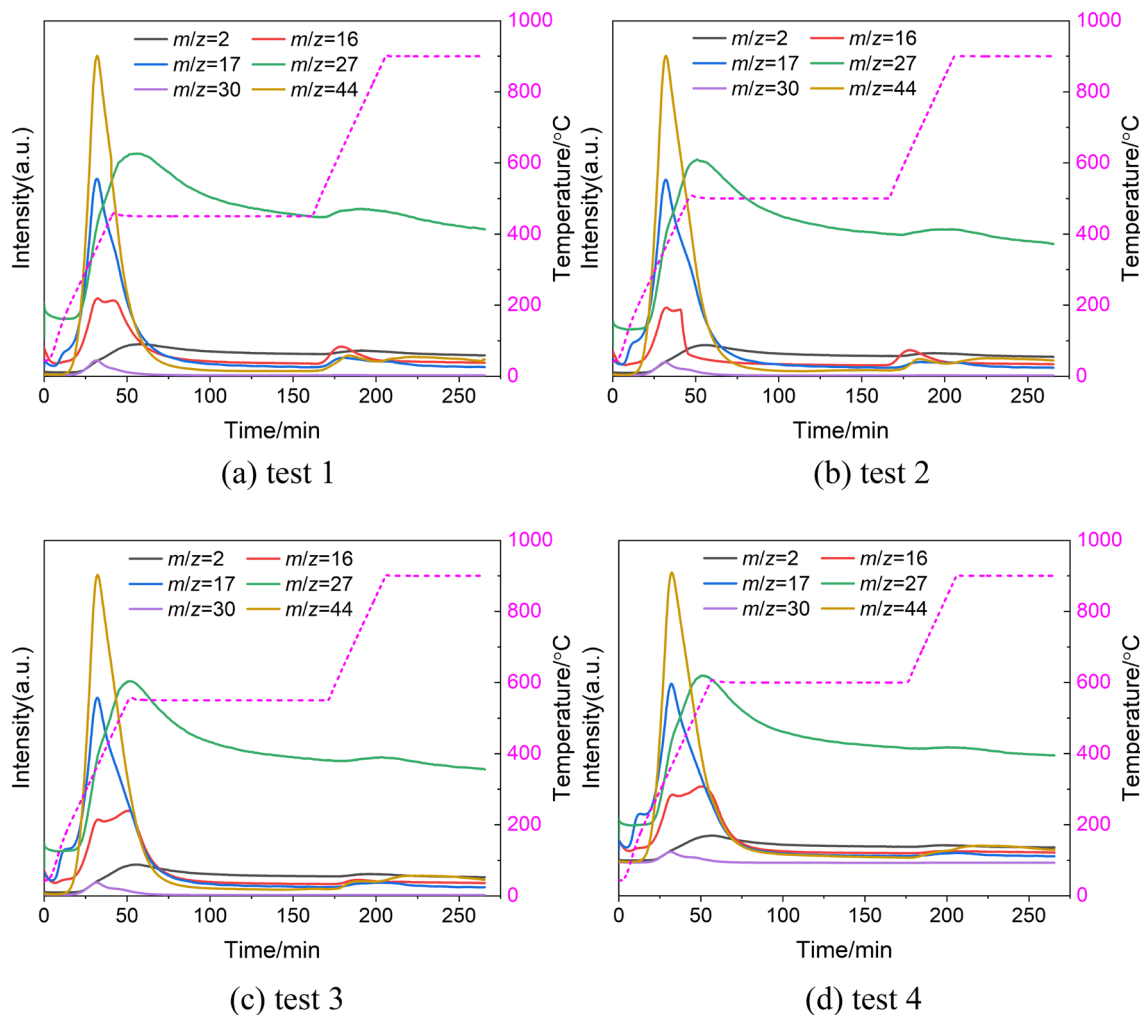


(a) test 1

(b) test 2

(c) test 3

(d) test 4

**Fig. 3** Gaseous products in different tests of TG-MS experiment

In the initial stage, due to the low reaction temperature, there is almost no escape of products. This stage corresponds to the first stage in the thermogravimetric curve, which is mainly the precipitation of free water and chemically bound water. In following stages of each test, the escape trends of the specific gaseous component are consistent in these tests, which results in the same mass spectrometry curves.

After more than ten minutes, the reaction temperature reaches above 150 °C, and the escape rate of each gas phase product increases, followed by the first peak of the $CO_2$, $C_3H_8$, $NH_3$, $CH_4$, and NO, $C_2H_4$. This is because the decomposition rates of hemicellulose, cellulose, and lignin in the solid phase reach a relatively high level. The peak temperature herein is consistent with the first peak temperature of DTG, which is within the range of 320–350 °C. Therefore, hemicellulose and cellulose decomposition products mainly include $CO_2$, $C_3H_8$, $NH_3$, $CH_4$, NO, and $C_2H_4$.

Subsequently, the reaction temperature of test 1 reached a constant range, while the temperature of test 2–4 continued rising, resulting in a secondary peak of $CH_4$ during this process. Due to the limitation of temperature, the $CH_4$ secondary peak in test 1 happens to be at the moment when the temperature rises to 450 °C, and in tests 2–4, the $CH_4$ secondary peak is also close to the moment when the pyrolysis temperature remains constant. It can be seen that temperature plays a decisive role in the $CH_4$ decomposition of hemicellulose, cellulose, and lignin. Under different operating conditions, the peak of HCN occurs at around 50 min, and there is no significant correlation between the peak time and the pyrolysis condition. As the pyrolysis reaction occurs, the peak of $H_2$ also appears after about 50 min.

In the subsequent constant temperature stage, the changes in the gas phase products are relatively slow, indicating that the pyrolysis reaction was quite complete in the previous heating stage. After 2 h, combustion of the pyrolysis biochar was conducted in an air atmosphere. At the beginning of heating up, each product begins to undergo significant changes. As the temperature increases, the curves of $CH_4$, HCN, $C_3H_8$, and $CO_2$ show peaks again. Although the gas phase products exhibit similar changing trends under different operating conditions, the pyrolysis temperature also has a significant impact on the peak value and change rate of the products.

In test 1, the pyrolysis temperature is lower, resulting in a relatively fast decrease rate of $NH_3$ and $C_3H_8/CO_2$ after the first peak. And the gas amount is relatively low which can be found from a narrower gas mass spectrometry peak. Similarly, the decrease rate of $CH_4$ peak also slows down at higher pyrolysis temperatures, indicating a high gas amount. From the HCN peak shown in Fig. 3, it can be more intuitively seen that during the combustion process with lower pyrolysis temperatures, the HCN peak is more pronounced. To further clarify the peak value of gas-phase products, a comparison between these tests was conducted on the product intensity during the combustion process, as shown in Fig. 4.

After pyrolysis, the residual from the contaminated biomass samples are burned in the air. Figure 3 shows that once combustion begins, the composition of the gas immediately begins to change, which can be intuitively reflected by the peak time in Fig. 4. During the combustion process, various gases were further released, resulting in more obvious peaks. It can be seen that except for $m/z = 44$, the peaks of other components show a decreasing trend from test 1 to test 4. This also indicates that in the early pyrolysis process, the residual content of C, H, N, O, and other elements in the solid products of low-temperature pyrolysis is relatively high, which is consistent with the thermogravimetric loss rate. For the gas phase component with $m/z = 44$, there were two peaks in the products of test 1, test 2, and test 3. The first peak appeared during the heating process, and the second peak appeared during the constant-temperature combustion. The peak value of this gas phase component in test 4 only appears during the combustion process. This further indicates that during the low-temperature pyrolysis process, carbon elements with relatively low bonding energy have not been fully decomposed, which may be due to incomplete decomposition of lignin.

## Pyrolysis kinetics of contaminated biomass sample

There have been many effective methods to obtain the pyrolysis kinetics, such as Fly-Wall-Ozawa (FWO), Kissinger-Akkahira-Sunose (KAS), Friedman method and so on. However, these methods need the multiple weight-loss rates. Kaczor et al. (2020) comprehensively reviewed the models of the biomass pyrolysis. In this work, it is seen that the one of the main objectives is to investigate the gas and solid products under different final pyrolysis temperatures. Therefore, in the TG-MS experiment, only one heating rate is employed. To calculate the kinetic parameters,
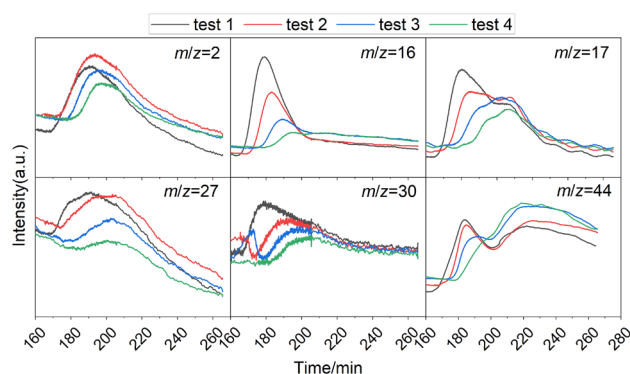


**Fig. 4** Comparison of gas products during the combustion process

a simple method, Coats-Redfern method is adopted in this work (Coats and Redfern 1964), which have also been used in other works focusing on the dispose of heavy metal-contaminated biomass (He et al. 2020). In the experiment, pyrolysis temperature changes with the heating time. During the experiment process, the pyrolysis rate can be described by the following equation:

$$\frac{d\alpha}{dt} = kf(\alpha) \tag{1}$$

in which, $k$ is the Arrhenius rate constant; $f(\alpha)$ is the reaction mechanism model; $t$ is reaction time; $\alpha$ is the conversion of biomass sample. In this work, the conversion $\alpha$ is the weight loss of the sample during pyrolysis.

According to the Arrhenius equation, reaction rate $k$ during pyrolysis should be

$$k = A \exp\left(-\frac{E_a}{RT}\right) \tag{2}$$

where, $A$ is the pre-exponential factor; $E_a$ is the apparent activation energy; $R$ is the gas constant, namely 8.314 J/(mol·K); $T$ is the temperature. Reaction mechanism model $f(\alpha)$ is not related to the time $t$ and temperature $T$, and it can be described as:

$$f(\alpha) = (1-\alpha)^n \tag{3}$$

where, $n$ is reaction order.

Then, Eq. (1) can be re-written as:

$$\frac{d\alpha}{dt} = A \exp\left(-\frac{E_a}{RT}\right)(1-\alpha)^n \tag{4}$$

In the experiment, the effect of pyrolysis temperature was investigated with the same heating rate. To obtain the pyrolysis kinetics in a relatively wide range, the experimental data in test 4 is adopted to calculate the kinetic parameters. The heating rate $\beta$ kept at 10 °C/min, which means the d$T$/d$t$ is constant. The conversion rate can be described as:

$$\frac{d\alpha}{dT} = \frac{A}{\beta} \exp\left(-\frac{E_a}{RT}\right)(1-\alpha)^n \tag{5}$$

By integrating the above equation, the following results can be obtained:

$$\ln\left[-\frac{\ln(1-\alpha)}{T^2}\right] = \ln\left[\frac{AR}{\beta E_a}\left(1-\frac{2RT}{E_a}\right)\right] - \frac{E_a}{RT} \quad (n=1) \tag{6}$$

$$\ln\left[\frac{1-(1-\alpha)^{1-n}}{(1-n)T^2}\right] = \ln\left[\frac{AR}{\beta E_a}\left(1-\frac{2RT}{E_a}\right)\right] - \frac{E_a}{RT} \quad (n \neq 1) \tag{7}$$

For convenience, Eqs. (6) and (7) are denoted as $Y = KX + b$ ($X = 1/T$). It is seen that $\ln\left[-\frac{\ln(1-\alpha)}{T^2}\right]$ or $\ln\left[\frac{1-(1-\alpha)^{1-n}}{(1-n)T^2}\right]$ should be linearly related to $1/T$ and the gradient is $-\frac{E_a}{R}$. To calculate the kinetic parameters, different values of n are adopted and the relationship between $Y$ and $X$ are shown in Fig. 5.

Although different orders have been tried, the relationship between $X$ and $Y$ is nonlinear in different cases. As illustrated in Fig. 2, at lower temperatures, because the dehydration process of the sample can cause certain errors, the pyrolysis kinetics calculation in this section does not consider the reaction kinetics of this process. In the second and third stages of pyrolysis, there is a significant nonlinear relationship between $Y$ and $X$ caused by different pyrolysis reactions.

As there were different reaction stages, the curves in the stages except for the evaporation of waster are divided into two sections according to the reaction temperature ranges. This concept was also used in other literatures (He et al. 2020). To accurately describe the reaction kinetics of each stage, the kinetic parameters of each stage are calculated, which is in line with the objective reaction process. Combining the results in Fig. 5, a linear function is used to fit different stages. When $n \leq 2$, the calculated apparent activation energy of the third stage is negative, which does not conform to its physical significance. When the reaction orders are 2.5 and 3, the fitting results are shown in Fig. 6.

As shown in Fig. 6, satisfactory fitting accuracy can be achieved by performing segmented linear fitting for different pyrolysis stages. By combining Eqs. (6) and (7), the kinetic parameters of different pyrolysis stages can be obtained, and the results are listed in Table 2.

The results indicate that at the second and third stages of pyrolysis, there are significant differences in kinetic parameters due to the different pyrolysis mechanisms. Regardless of whether the reaction order is 2.5 or 3, the apparent activation energy of the second stage is much greater than that of
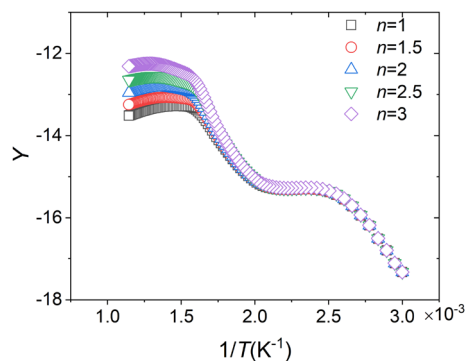


**Fig. 5** Relationships between $X$ and $Y$ with different reaction orders

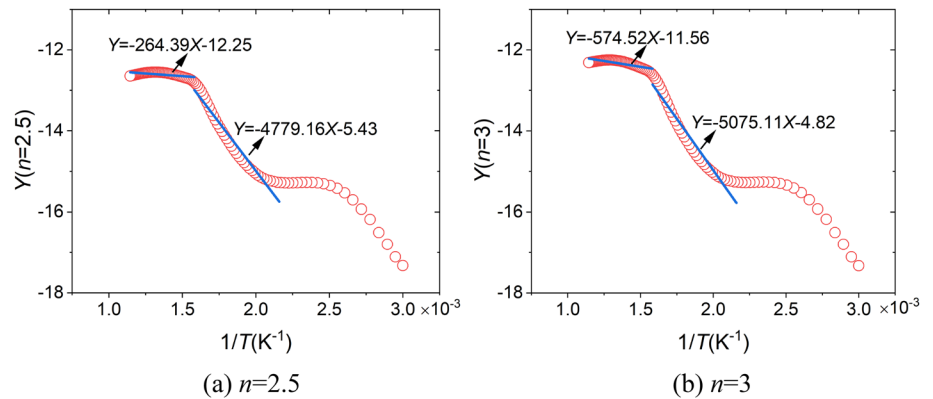**Fig. 6** *Y* and *X* fitting results of pyrolysis stages with different orders



(a) *n*=2.5

(b) *n*=3

**Table 2** Kinetic parameters of different pyrolysis stages

| Parameter | *n*=2.5 | | *n*=3 | |
|---|---|---|---|---|
| | Second stage | Third stage | Second stage | Third stage |
| $E_a$ (kJ/mol) | 39.73 | 2.20 | 42.04 | 4.78 |
| $A$ (min$^{-1}$) | 209.10 | 0.013 | 406.58 | 0.055 |

the third stage. At the same time, it can be seen that the pre-exponential factor in the second stage is also much greater than that in the third stage. He et al. (2020) used the same method to investigate the pyrolysis kinetics, which divided the temperature range into 200–340 °C and 350–530 °C for the linearity fitting. The apparent activation energies of the raw biomass are 68.28 kJ/mol and 67.83 kJ/mol in these ranges, which are higher than those of the material in this work.

## Retention characteristics of heavy metals

As the mass of pyrolyzed biochar in TG is quite low, the pyrolysis experiment was conducted in a fixed bed reactor with the same conditions as the TG pyrolysis experiment to obtain more biochar for analyses. In each test, a 1.0000 g biomass sample was placed in the fixed bed reactor, and then it was heated to pyrolysis temperatures (450, 500, 550, and 600 °C) with a specific rate of 10 °C/min. Then, the temperature was kept for 2 h. After that, the pyrolysis product was cooled in the $N_2$ atmosphere. Under different conditions, the weight loss in pyrolysis is shown in Fig. 7.

It is seen that the weight loss increases against pyrolysis temperature in different reactors. Commonly, the weight loss in TG is slightly lower than that in a fixed-bed reactor at the same pyrolysis temperature. In a fixed bed reactor, the gas stream may carry a part of fine sample powder while it can not take place in TG. This should be the reason why the weight loss in the fixed bed reactor is higher than that in TG. In addition, the tar produced in pyrolysis using TG can not be carried out while it flows downstream of the fixed bed
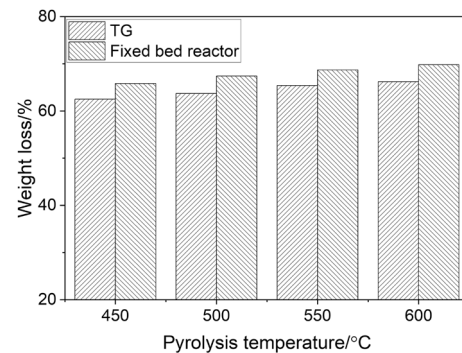


**Fig. 7** Weight loss of biomass sample during the pyrolysis process

reactor. The weight loss differences between TG and fixed bed reactor experiments are very close, demonstrating the pyrolysis experiment's reliability. To investigate the retention of Cu and Mn in contaminated biomass, the pyrolyzed biochar from a fixed-bed reactor was analyzed. The contents and retention rates of Cu and Mn in biochar are shown in Fig. 8.

Results in the figure demonstrate that both the content and retention rate decrease with the climb of pyrolysis temperature. The concentrations of Cu and Mn in biochar are much higher than those in the raw samples. That means pyrolysis is beneficial to the enrichment of Cu and Mn in solid products. The concentration of Cu shows an obvious decrease between 450 and 500 °C. And their retention rates also decrease in this range. When the pyrolysis temperature increases from 450 °C to 600 °C, the retention rate of Cu decreases from 64.6% to 26.4% while that of Mn decreases from 58.8% to 34.4%.

## Conclusion

To utilize the resource of contaminated biomass, a two-stage thermochemical method was employed to dispose of it. Based on this concept, pyrolysis and combustion

**Fig. 8** Contents and retention rates of Cu and Mn in biochar



(a) Cu        (b) Mn
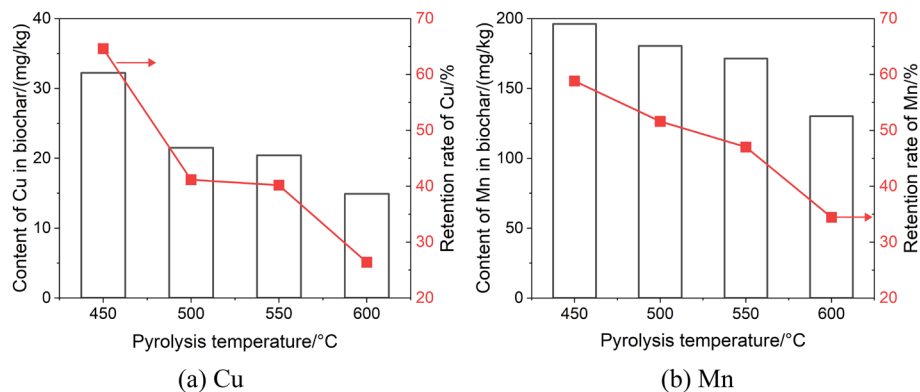
performances are investigated in TG-MS and a fixed-bed reactor to identify the products behaviors. Following conclusions can be drawn from the results:

(1) The results indicate that low-temperature pyrolysis can improve carbon retention and facilitate the enrichment of Cu and Mn in solid products. TG and fixed-bed pyrolysis experiments have similar levels of sample weight loss.

(2) When the pyrolysis temperature increases from 450 ℃ to 600 ℃, the retention rate of Cu in the solid phase decreases from 64.6% to 26.4%, while the retention rate of Mn decreases from 58.8% to 34.4%.

(3) In the second stage of the pyrolysis process, the apparent activation energy of the pyrolysis reaction is 39.73–42.04 kJ/mol, while the apparent activation energy of the third stage is much lower than that of the second stage, which is about 2.20–4.78 kJ/mol.

Further investigation is needed to investigate the behavior of heavy metals in biochar during the combustion process.

## Declarations

**Conflict of interest** The authors declare that they have no known competing financial interests or personal relationships that could have appeared to influence the work reported in this paper.

**Ethical approval** Research does not report on or involve the use of any animal or human data or tissue.

**Consent to participate** Not applicable.

**Consent for publication** All the authors gave consent for the publication of this journal.

## References

Amabogha ON, Garelick H, Jones H, Purchase D (2023) Combining phytoremediation with bioenergy production: developing a multi-criteria decision matrix for plant species selection. Environ Sci Pollut Res 30:40698–40711

Chai Y, Bai M, Chen A, Peng L, Shao J, Shang C, Peng C, Zhang J, Zhou Y (2022) Thermochemical conversion of heavy metal contaminated biomass: fate of the metals and their impact on products. Sci Total Environ 822:153426

Coats AW, Redfern JP (1964) Kinetic parameters from thermogravimetric data. Nature 201(4914):68–69

Du J, Zhang L, Ali A, Li R, Xiao R, Guo D, Liu X, Zhang Z, Ren C, Zhang Z (2019) Research on thermal disposal of phytoremediation plant waste: stability of potentially toxic metals (PTMs) and oxidation resistance of biochars. Process Saf Environ Prot 125:260–268

Grottola CM, Giudicianni P, Pindozzi S, Stanzione F, Faugno S, Fagnano M, Fiorentino N, Ragucci R (2019) Steam assisted slow pyrolysis of contaminated biomasses: effect of plant parts and process temperature on heavy metals fate. Waste Manage 85:232–241

He J, Strezov V, Kan T, Weldekidan H, Asumadu S, Kumar R (2019a) Effect of temperature on heavy metal (loid) deportment during pyrolysis of Avicennia marina biomass obtained from phytoremediation. Biores Technol 278:214–222

He J, Strezov V, Kumar R, Weldekidan H, Jahan S, Dastjerdi BH, Zhou X, Kan T (2019b) Pyrolysis of heavy metal contaminated Avicennia marina biomass from phytoremediation: characterisation of biomass and pyrolysis products. J Clean Prod 234:1235–1245

He J, Strezov V, Zhou X, Kan T, Kumar R (2020) Effect of phosphate pretreatments on properties of pyrolytic products from heavy-metal-contaminated biomass. Energy Fuels 34:15322–15331

He D, Hu H, Jiao F, Zuo W, Liu C, Xie H, Dong L, Wang X (2023) Thermal separation of heavy metals from municipal solid waste incineration fly ash: a review. Chem Eng J 467:143344

Hou D, O'Connor D, Igalavithana A, Alessi D, Luo J, Tsang D, Sparks D, Yamauchi Y, Rinklebe J, Ok Y (2020) Metal contamination and

bioremediation of agricultural soils for food safety and sustainability. Nat Rev Earth Environ 1:366–381

Huang H, Yao W, Li R, Ali A, Du J, Guo D, Xiao R, Guo Z, Zhang Z, Awasthi M (2018) Effect of pyrolysis temperature on chemical form, behavior and environmental risk of Zn, Pb and Cd in biochar produced from phytoremediation residue. Biores Technol 249:487–493

Kaczor Z, Bulinski Z, Werle S (2020) Modelling approaches to waste biomass pyrolysis: a review. Renew Energy 159:427–443

Kovacs H, Szemmelveisz K (2017) Disposal options for polluted plants grown on heavy metal contaminated brownfield lands-a review. Chemosphere 166:8–20

Kuppens T, Dael MV, Vanreppelen K, Thewys T, Yperman J, Carleer R, Schreurs S, Passel S (2015) Techno-economic assessment of fast pyrolysis for the valorization of short rotation coppice cultivated for phytoextraction. J Clean Prod 88:336–344

Lee J, Park KY (2021) Conversion of heavy metal-containing biowaste from phytoremediation site to value-added solid fuel through hydrothermal carbonization. Environ Pollut 269:116127

Lievens C, Yperman J, Vangronsveld J, Carleer R (2008a) Study of the potential valorisation of heavy metal contaminated biomass via phytoremediation by fast pyrolysis: part I. Influence of temperature, biomass species and solid heat carrier on the behaviour of heavy metals. Fuel 87:1894–1905

Lievens C, Yperman J, Cornelissen T, Carleer R (2008b) Study of the potential valorisation of heavy metal contaminated biomass via phytoremediation by fast pyrolysis: part II: characterisation of the liquid and gaseous fraction as a function of the temperature. Fuel 87(10–11):1906–1916

Liu Z, Tran KQ (2021) A review on disposal and utilization of phytoremediation plants containing heavy metals. Ecotoxicol Environ Saf 226:112821

Liu WJ, Tian K, Jiang H, Zhang X, Ding H, Yu H (2012) Selectively improving the bio-oil quality by catalytic fast pyrolysis of heavy-metal-polluted biomass: take copper (Cu) as an example. Environ Sci Technol 46(14):7849–7856

Liu Z, Wang L, Xiao H, Guo X, Urbanovich O, Nagorskaya L, Li X (2020) A review on control factors of pyrolysis technology for plants containing heavy metals. Ecotoxicol Environ Saf 191:110181

Raheem A, He Q, Mangi F, Areeprasert C, Ding L, Yu G (2022) Roles of heavy metals during pyrolysis and gasification of metal-contaminated waste biomass: a review. Energy Fuels 36(5):2351–2368

Shah V, Daverey A (2020) Phytoremediation: a multidisciplinary approach to clean up heavy metal contaminated soil. Environ Technol Innov 18:100774

Stals M, Thijssen E, Vangronsveld J, Carleer R, Schreurs S, Yperman J (2010) Flash pyrolysis of heavy metal contaminated biomass from phytoremediation: influence of temperature, entrained flow and wood/leaves blended pyrolysis on the behaviour of heavy metals. J Anal Appl Pyrol 87(1):1–7

Sun C, Ding D, Chen T, Huang Q, Lu S, Yan J (2019) Ecological risk analysis of the solid residues collected from the thermal disposal process of hyperaccumulator *Pteris vittata* including heavy metals and environmentally persistent free radicals. Environ Sci Pollut Res 26:29234–29245

Tran K, Werle S, Trinh T, Magdziarz A, Sobek A, Pogrzeba M (2020) Fuel characterization and thermal degradation kinetics of biomass from phytoremediation plants. Biomass Bioenerg 134:105469

Wang S, Gao B, Li Y, Yong Ok, Shen C, Xue S (2017) Biochar provides a safe and value-added solution for hyperaccumulating plant disposal: a case study of Phytolacca acinosa Roxb. (Phytolaccaceae). Chemosphere 178:59–64

Wang X, Huang Y, Shao Y, Zhu J, Jin B (2022) Thermodynamic evaluation on chemical looping conversion of Cd-and Zn-contained phytoremediation plant with different CaO pathways. Chemosphere 292:133433

Wang Q, Huang S, Jiang R, Zhuang Z, Liu Z, Wang Q, Wan Y, Li H (2023a) Phytoremediation strategies for heavy metal-contaminated soil by selecting native plants near mining areas in Inner Mongolia. Environ Sci Pollut Res 30:94501–94514

Wang X, Shao Y, Wang R, Jin B (2023b) Experimental investigation on the separated gasification chemical looping combustion performance of phytoremediation plant and retention of heavy metals. Fuel 343:127880

Wiangkham N, Prapagdee B (2018) Potential of Napier grass with cadmium-resistant bacterial inoculation on cadmium phytoremediation and its possibility to use as biomass fuel. Chemosphere 201:511–518

Wu Y, Li X, Yu L, Wang T, Wang J, Liu T (2022) Review of soil heavy metal pollution in China: spatial distribution, primary sources, and remediation alternatives. Resour Conserv Recycl 181:106261

Zeng K, Li R, Minh D, Weiss-Hortala E, Nzihou A, He X, Flamant G (2019) Solar pyrolysis of heavy metal contaminated biomass for gas fuel production. Energy 187:116016

Zhang Y, Chen Z, Xu W, Liao Q, Zhang H, Hao S, Chen S (2020) Pyrolysis of various phytoremediation residues for biochars: chemical forms and environmental risk of Cd in biochar. Biores Technol 299:122581

Zhang J, Wu S, Xu J, Liang P, Wang M, Naidu R, Liu Y, Man Y, Wong M, Wu S (2021a) Comparison of ashing and pyrolysis treatment on cadmium/zinc hyperaccumulator plant: effects on bioavailability and metal speciation in solid residues and risk assessment. Environ Pollut 272:116039

Zhang Y, Chen Z, Chen C, Li F, Shen K (2021b) Effects of UV-modified biochar derived from phytoremediation residue on Cd bioavailability and uptake in *Coriandrum sativum* L. in a Cd-contaminated soil. Environ Sci Pollut Res 28:17395–17404